

First-in-first-out item replacement in a model of  
short-term memory based on persistent spiking

Randal A. Koene and Michael E. Hasselmo

Center for Memory and Brain

Department of Psychology and Program in Neuroscience

Boston University

64 Cummington Street, Boston, MA 02215, U.S.A.

tel: 1-617-358-2769, fax: 1-617-353-1424

randalk@bu.edu

February 25, 2006

**Abstract**

Persistent neuronal firing has been modeled in relation to observed brain rhythms, especially to theta oscillations recorded in behaving animals. Models of short-term memory that are based on such persistent firing properties of specific neurons can meet the requirements of spike-timing dependent potentiation of synaptic strengths during the encoding of a temporal sequence of spike patterns. We show that such a spiking buffer can be simulated with integrate-and-fire neurons that include a leak current, even when different numbers of spikes represent successive items. We propose a mechanism that successfully replaces items in the buffer in first-in-first-out order when the distribution of spike density in a theta cycle is asymmetric, as found in experimental data. We predict effects on the function and capacity of the buffer model caused by changes in modeled theta cycle duration, the timing of input to the buffer, the strength of recurrent inhibition, and the strength and timing of after-hyperpolarization and after-depolarization. Shifts of input timing or changes in after-depolarization parameters can enable the reverse order buffering of items, with first-in-first-out replacement in a full buffer. As noise increases, the simulated buffer provides robust output that may elicit episodic encoding.

**Keywords:** Short-term memory, persistent firing, integrate-and-fire neurons, theta rhythm, gamma rhythm, sequence buffer

Computer simulations of the encoding of a temporal sequence of spike patterns in recurrent neuronal networks often rely on a Hebbian model (Hebb, 1949) of spike timing dependent potentiation (STDP) for the update of synaptic strengths. During learning, these simulations depend on the repeated presentations of spike patterns that are separated by time intervals smaller than about 40 ms, a window within which consecutive pre- and postsynaptic spikes were found to elicit long-term potentiation (Levy and Stewart, 1983; Markram *et al.*, 1997; Bi and Poo, 1998). Yet in realistic experiments a subject may be exposed to a sequence of stimuli that are separated by greater time intervals. One way to deal with this problem is to store each sequence in a short-term buffer that presents items at appropriate intervals. Since such a buffer cannot depend on synaptic modification for the temporary storage, we presuppose a mechanism of persistent spiking. The mechanism relies on after-depolarization (ADP), a membrane response that is intrinsic to many pyramidal cells of the entorhinal cortex (Klink and Alonso, 1997a,b; Egorov *et al.*, 2002).

Computer models by Lisman and Idiart (1995) and Jensen *et al.* (1996) have simulated short-term memory (STM) function based on persistent spiking during modulation by theta rhythm. Previous simulations based on these models did not deal with the dynamic characteristics of leaky spiking neurons and provided no mechanism for the ordered replacement of items in a buffer that is filled to capacity. In prior work, we proposed buffer models that are related to those STM models based on persistent spiking, yet more accurately simulate the asymmetric distribution of spiking activity in each cycle of the 3-12 Hz theta brain rhythm (Koene, 2006b,a) and that simulate neuronal dynamics using leaky integrate-and-fire neurons (Koene *et al.*, 2003). The implementation of the more realistic asymmetry has functional benefits: Distinct portions of each theta cycle in a buffer can be synchronized with distinct modes of synaptic encoding

and retrieval that alternate in each cycle of a theta rhythm in the recurrent networks that receive spike input from that buffer (Koene *et al.*, 2003; Koene and Hasselmo, 2005). By contrast, Jensen *et al.* (1996) relied on temporally separated periods of at least several seconds that are devoted exclusively to associative encoding or to retrieval in order to avoid interference between spiking in those two modes. Here, we add to the model a plausible mechanism for the first-in-first-out (FIFO) ordered replacement of items that are maintained in the buffer as successive patterns of simultaneous spikes. While Jensen *et al.* (1996) described a method by which items in the buffer could be replaced as new input appears, that proposal was not evaluated in simulations and their proposed method relied on an even distribution of item reactivation spikes throughout a theta cycle. The mechanism proposed here performs the ordered replacement of buffered items, even when different numbers of simultaneous spikes represent each item, as may be expected for realistic stimuli. Our previously published studies involved the extensive use of an integrate-and-fire version of the STM buffer model in which pattern reactivation occurs specifically at the depolarized phase of theta modulation. Those studies focused on hippocampal (Koene *et al.*, 2003; Hasselmo *et al.*, 2002b) and prefrontal cortex function (McGaughy *et al.*, 2005; Koene and Hasselmo, 2005) during behavioral tasks in which the results of neuronal computation elicited dynamic responses from the task environment, but did not deal specifically with the issue of patterns with different numbers of simultaneous spikes that represent the items maintained in STM.

Different numbers of neurons may spike to represent (a) the last item reactivated in the ordered buffer, (b) the insertion of a new item into the buffer by input and (c) the first item that may need to be removed from the buffer. A process of item replacement is therefore needed, which depends on whether any number of spikes occur in the last item phase of the buffer cycle (Fig. 1a) as well

as any number of spikes occur at the input phase of the buffer cycle (Fig. 1b). That process must suppress an arbitrary number of spikes at that phase of the buffer cycle, when the spikes of the first item would be reactivated (Fig. 1c).

- Figure 1 about here -

In the following sections we describe the STM buffer model, as implemented in the Catacomb (Cannon *et al.*, 2003) simulation environment and its performance with different numbers of spikes representing individual items. The mechanism postulated for first-in-first-out replacement of buffered items is then presented. The functional effects of significant changes of specific parameters of the STM model are analyzed, and modifications that lead to first-in-first-out buffering in the reversed order of item presentation are demonstrated. Finally, the buffer model is shown to exhibit sufficient robustness in the presence of increasing levels of noise that affect spike timing, to act as a useful short-term memory when novel items need to be sustained for encoding in episodic memory.

## 1 METHODS

We presuppose that many pyramidal cells in layer II of entorhinal cortex (ECII) are specifically suited to reactivate firing patterns in a persistent manner due to intrinsic neuronal mechanisms. Such neurons exhibit an after-depolarization (ADP) of membrane potential after an action potential is elicited at the membrane. Klink and Alonso (1997a) showed that the ADP is caused by calcium sensitive cation currents that are induced by muscarinic receptor activation. In addition to the ADP, activity in EC is modulated by a strong brain rhythm known as the theta rhythm that is present in behaving animals (Buzsáki *et al.*, 1983; Fox, 1989; Fox *et al.*, 1986). In rats for example, the theta rhythm has a frequency of about 8 Hz. This rhythm may synchronize activity within a short-term memory based on persistent spiking (Koene *et al.*, 2003), and it

may synchronize output to other regions such as region CA3 (Hasselmo *et al.*, 2002a) or layer III of EC (Koene *et al.*, 2003), where corresponding synaptic changes may occur. The reactivation of firing patterns by ADP in an ECII population of neurons between specific phases of each cycle of theta rhythm can therefore provide reliable input to other neuronal populations. Our model of short-term memory (STM) in EC builds on a model first proposed by Lisman and Idiart (Lisman and Idiart, 1995; Jensen and Lisman, 1996a). In both models, recurrent inhibition separates the reactivation of sequential spike patterns in the buffer. The inhibition is provided by a population of interneurons, all of which spike in response to an action potential at any pyramidal cell in ECII (Bragin *et al.*, 1995).

### **A leaky integrate-and-fire neuron implementation of the short-term memory buffer**

Equation 1 shows how various contributions affect the response of model ECII pyramidal neurons, and therefore their ability to sustain ordered sequences of spikes.

$$C\Delta v = \sum_i (g_i \Delta t (E_{rev,i} - (V + \Delta v))), \quad (1)$$

which can be rewritten as

$$\Delta v = \frac{\sum_i (g_i \Delta t (E_{rev,i} - V))}{C + \sum_i (g_i \Delta t)}, \quad (2)$$

where  $C$  is the membrane capacitance,  $\Delta v$  is the change of the membrane potential  $V$  during a small time interval  $\Delta t$ , and  $g_i$  is the conductance and  $E_{rev,i}$  the reversal potential of a contributing membrane current. Below, we describe the contributing currents provided by rhythmic theta modulation, external afferent input to the buffer cells, intrinsic after-hyperpolarizing and after-depolarizing

responses to action potentials, and inhibitory synaptic input from recurrent fibres of an interneuron network that is responsible for the observed gamma rhythm.

We use integrate-and-fire simulations of pyramidal cells of ECII, which have a membrane response with exponential decay to a resting potential  $E_{rest} = -60$  mV due to membrane capacitance of  $C = 1$  mF and time constant of the leak conductance  $\tau_{leak} = 9$  ms<sup>1</sup>. The current contributed to the membrane potential by the leak conductance is defined by  $E_{rest}$  and the conductance  $g_{leak} = C/\tau_{leak}$ . The firing threshold is  $-50$  mV, and the resting potential of  $-60$  mV is chosen as the reset potential that follows a spike. Action potentials have a duration of 1 ms and are followed by a 2 ms refractory period and subsequent strong after-hyperpolarization (AHP). Many currents in Eq. 2, such as the AHP and synaptic input are simulated with a fixed reversal potential  $E_{rev,i}$  and a bi-exponential conductance response function

$$g_i(t) = G_i a_{norm} (\exp(-t/\tau_{fall,i}) - \exp(-t/\tau_{rise,i})), \quad (3)$$

where  $G_i$  is the characteristic amplitude of the conductance response for a specific membrane current,  $\tau_{fall,i}$  and  $\tau_{rise,i}$  are its fall and rise time constants and  $a_{norm}$  is a normalizing factor to insure that the maximum value of  $g_i(t)$  is  $G_i$ . The normalizing factor is computed by

$$a_{norm} = 1/(\exp(-t_{max}/\tau_{fall,i}) - \exp(-t_{max}/\tau_{rise,i})), \quad (4)$$

---

<sup>1</sup>The STM buffer has been shown to work with time leak constants between 8 ms and 19 ms. Below 8 ms, spike reactivation does not occur, while spikes may reactivate twice in one theta period when the time constant is above 19 ms, which leads to changes in the order of the spike patterns that are sustained in the buffer.

where the time offset of the maximum response value is

$$t_{max} = \ln\left\{\frac{\tau_{fall,i}/\tau_{rise,i}}{(1/\tau_{rise,i}) - (1/\tau_{fall,i})}\right\}. \quad (5)$$

The AHP response approximates a single exponential function through a small rise time constant  $\tau_{rise,AHP} = 10^{-4}$  ms and an exponential decay time constant  $\tau_{fall,AHP} = 30$  ms with amplitude  $G_{AHP} = 23$  nS, and has a reversal potential of  $E_{AHP} = -90$  mV. The bi-exponential ADP response has the shape of an alpha function with time constants  $\tau_{rise,ADP} = \tau_{fall,ADP} = 125$  ms, amplitude  $G_{ADP} = 30$  nS and the reversal potential  $E_{ADP} = -45$  mV. The ADP must rise over a time span that is approximately equal to the period of a theta cycle, since reactivation of spikes on the rising flank of the ADP response insures that the order of spiking is maintained.

We model the rhythmic oscillation of the membrane potentials of pyramidal cells in ECII as inhibitory synaptic input that is modulated by rhythmic activity at a frequency of 8 Hz originating in the medial septum (Alonso *et al.*, 1987; Stewart and Fox, 1990; Skaggs *et al.*, 1996; Wallenstein and Hasselmo, 1997; Brazhnik and Fox, 1999). The bi-exponential synaptic responses that cause this modulation have reversal potential  $E_{theta} = -90$  mV, a conductance amplitude of  $G_{theta} = 10$  nS and time constants  $\tau_{rise,theta} = 0.1$  ms and  $\tau_{fall,theta} = 20$  ms. This gives the modulation of membrane potential the typical asymmetrical shape of the theta rhythm. The simulated 8 Hz theta rhythm is driven by septal spikes that commence at  $t = 0$  ms.

An interneuron population in ECII is simulated by a single interneuron that receives fast connections<sup>2</sup> from all pyramidal buffer cells and provides recurrent input to all pyramidal buffer cells. The interneuron responds rapidly to any buffer output spikes, due to bi-exponential synaptic input with the character-

---

<sup>2</sup>Fast connections are simulated with a transmission delay of between 0 ms and 1 ms.

istic parameters  $G = 30$  nS,  $\tau_{rise} = 1$  ms and  $\tau_{fall} = 2$  ms, and a postsynaptic reversal potential  $E_{rev} = 0$  mV. This “gamma” interneuron recuperates quickly due to a fast AHP response with  $E_{AHP} = -90$  mV,  $G_{AHP} = 100$  nS,  $\tau_{rise,AHP} = 10^{-4}$  ms and  $\tau_{fall,AHP} = 4$  ms. The interneuron model differs from that of the pyramidal cells due to reset and rest potentials  $E_{reset} = E_{rest} = -70$  mV and a leak time constant  $\tau_{leak} = 10$  ms. The competitive inhibition provided to pyramidal buffer cells by the model interneuron population simulates the postsynaptic response of  $GABA_A$  receptors as a membrane current with  $E_{gamma} = -70$  mV, and a bi-exponential conductance response with characteristic parameters  $G_{gamma} = 100$  nS,  $\tau_{rise,gamma} = 0.1$  ms and  $\tau_{fall,gamma} = 2.5$  ms.

The transmission of new input spikes to the buffer, as well as the transmission of recurrent inhibition that is observed as a power variation in the gamma frequency band of the EEG are modulated at theta frequency due to  $GABA_B$  receptor activation by septal input at presynaptic terminals. In our simulations, the dynamic shape of the modulating amplitude,  $f_{tmod}(t)$ , is generated by the normalized output of a model neuronal membrane that receives synaptic input at theta frequency. The resulting transmission modulation has a scalloped shape typical of observed theta modulation. The transmission modulated conductance responses of input ( $g_{input}(t)f_{tmod,input}(t)$ ) and of recurrent inhibition ( $g_{gamma}(t)f_{tmod,gamma}(t)$ ) are 180 degrees out of phase. This means that input is suppressed during the reactivation phase of the buffer, at which time recurrent inhibition is needed to maintain the separation of successive spike patterns. Conversely, recurrent inhibition is suppressed when new input is received at the input phase of the buffer (which may initiate item replacement if the buffer is full). The period of greatest depolarization due to membrane currents produced by the theta rhythm (with  $E_{theta}$  and  $g_{theta}(t)$ ) is in phase with the strongest

recurrent inhibitory transmission from the gamma interneuron population.

As in Lisman and Idiart (1995), spikes produced in ECII by stimulus input are reactivated repeatedly by the combination of ADP and positive theta modulation of membrane potential at a rate that matches the frequency of theta oscillation. A pattern of spikes that represents a stimulus input is maintained by this persistent spiking without any prerequisite synaptic connectivity. The reactivation of a spike by ADP is shown in figure 2. Rhythmic septal spikes that initiate each cycle of the membrane oscillation and the modulation of afferent and recurrent transmission have a 112 ms offset, while the first afferent can appear at  $t = 125$  ms (i.e. input appears with a 13 ms relative phase offset after the peak of theta depolarization). The phase offset of all rhythmic input or modulation in the following paragraphs is given as an offset from  $t = 0$  ms.

- Figure 2 about here -

The membrane potentials of three neurons of a STM buffer are plotted in figure 3. Theta oscillations define two functional phases of the buffer neurons. We call the phase interval of greatest rhythmic depolarization the reactivation phase of STM and the remaining interval the input phase of STM. The plots show that spiking produced by afferent activity during the input phase of the buffer is reactivated by the ADP during subsequent reactivation phases. The duration of the rise of ADP matches the period of oscillation. This means that the ADP of the earliest neuron to spike in one cycle allows that neuron to reach threshold first in the following cycle. The order of spikes is maintained during reactivation in STM. As spikes caused by output of the buffer occur in pre- and postsynaptic neurons of a target population with recurrent fibres such as entorhinal layer III or region CA3 of the hippocampus, an asymmetric function of spike-timing dependent potentiation (STDP) can take into account the order of spikes. This ensures that LTP (Bliss and Lømo, 1973; Bliss and Collingridge,

1993) is elicited in specific connections so that the order of events is maintained in episodic memory.

- Figure 3 about here -

A rapid succession of septal spikes is used to suppress action potentials in the buffer neurons between trials of an experiment. This simulates the disappearance or resetting of theta rhythm as observed during context switches (Wyble *et al.*, 2004). The buffer is cleared for the next trial.

### **A phase-locked mechanism of first-in-first-out replacement of buffered items**

In the absence of input, the contents of a STM buffer decay gradually, due to noise and a slow-AHP (modeled as a bi-exponential response with  $E_{rev} = -70$  mV,  $G = 0.01$  nS,  $\tau_{rise} = \tau_{fall} = 3000$  ms, an alpha function). When a buffer that is filled to capacity receives new input at a rapid pace, so that neither the loss of spikes due to effects of noise or due to slow-AHP remove items from the buffer before the new input arrives, continued ordered buffering of the most recent spike patterns is only possible if a mechanism exists that can selectively remove the representation of the first item from the buffer to make room for a representation of the new item. If each item can be represented by a different number of simultaneous spiking pyramidal cells in the buffer, then the mechanism must be able to remove the first item regardless of how many and which neurons spiked to represent that item, and it must do this only when the buffer is full and new input arrives<sup>3</sup>. Neither the arrival of new input or the “full” state of the buffer can be determined simply by detecting the activity of a certain number of spikes within a given time interval, since the representations of the afferent input and of the reactivated items in the buffer may each consist

---

<sup>3</sup>If the buffer state is not detected and item replacement is elicited for every afferent input then the effective buffer has the capacity to maintain one item.

of any number of spikes. In a buffer that depends on the timing of input and of gamma sub-cycles within each theta cycle, a reliable indicator of “full” buffer state and of an input event is the presence of spikes at specific phases of the theta cycle. In particular, spikes at the input phase of the theta cycle indicate the arrival of new afferent input and spikes at the reactivation phase of the Nth item in a buffer with a capacity of N items indicate that the buffer is filled to capacity.

We therefore propose a first-in-first-out ordered item replacement mechanism for the short-term memory buffer that is robust with regard to differences in the number of spikes that represent specific items in the buffer. Our model for the replacement mechanism assumes that in addition to cells with ADP ( $P_{ADP}$  in Fig. 4) ECII contains at least three other functionally distinct populations of neurons (schematically drawn as single nodes in Fig. 4, all with  $E_{rest} = E_{reset} = -60$  mV). These are two populations of pyramidal cells (Pf and Pi in Fig. 4, both with  $\tau_{leak} = 9$  ms and bi-exponential fast AHP responses with  $E_{rev} = -90$  mV,  $G = 10$  nS,  $\tau_{rise} = 0.1$  ms and  $\tau_{fall} = 50$  ms) that do not exhibit after-depolarization and one population of interneurons (Ir in Fig. 4, with  $\tau_{leak} = 10$  ms) that is not already recruited to participate in the recurrent gamma inhibition.

- Figure 4 about here -

Pyramidal cells of the Pf population receive as input (with bi-exponential postsynaptic responses at each synapse specified by  $E_{rev} = 0$  mV,  $G = 6$  nS,  $\tau_{rise} = 0.1$  ms and  $\tau_{fall} = 1$  ms) the spikes produced by the pyramidal buffer cells (input spikes C in Fig. 4). That input is transmission modulated by activity on  $GABA_B$  receptors on the terminals of the input synapses (depicted as the modulation B given to node Tm in Fig. 4) so that the input gated in this manner is sensitive to the specific phase interval at which the reactivation of the Nth item

in the buffer normally occurs. The membrane potential of pyramidal cells in Pf is also modulated by theta rhythm (due to inhibitory bi-exponential responses with  $E_{rev} = -90$  mV,  $G = 10$  nS,  $\tau_{rise} = 0.1$  ms and  $\tau_{fall} = 20$  ms) at the same phase as the modulation of the pyramidal cells that provide persistent spiking in the buffer. The synaptic strength of buffer input to the Pf population is tuned to cause spikes in Pf when one or more postsynaptic potentials are elicited, while the after-hyperpolarization of the Pf neurons prevents bursting when many simultaneous inputs are received. The Pf population functions as a “full” buffer state detector that is independent of the number of spikes that are reactivated during each theta cycle of the buffer, as demonstrated by the membrane response D in Fig. 4.

The capacity of the buffer is constrained by the phase offset of the transmission modulation that determines the Nth item reactivation phase at which the Pf population detects a full buffer. In our implementation with an 8 Hz theta rhythm, the buffer is able to maintain up to five items (with some restrictions on the input protocol, as explained in the Discussion), and this maximum capacity is specified by a phase offset of 103 ms. A phase offset of 84 ms limits the capacity to four items, which is a robust capacity for this buffer. With a phase offset of 68 ms, the buffer capacity is limited to three items<sup>4</sup>.

Pyramidal cells of the Pi population receive as input (with  $E_{rev} = 0$  mV,  $G = 6$  nS,  $\tau_{rise} = 0.1$  ms and  $\tau_{fall} = 1$  ms) the spikes that provide afferent input to the buffer (E in Fig. 4). Pi neurons also receive rhythmic excitatory input at theta frequency (with  $E_{rev} = 0$  mV,  $G = 2$  nS,  $\tau_{rise} = 0.1$  ms and  $\tau_{fall} = 20$  ms) that is synchronized with the theta modulation of buffer pyramidal cells (F in Fig. 4). This depolarization and the strength of synaptic input due to afferent buffer input spikes are tuned so that Pi neurons spike when one or more afferent

---

<sup>4</sup>In order to allow for some variability of spike timing, which includes the possibility of earlier spiking, the phase offsets were chosen to be 4 ms before the greatest offset at which a full buffer is consistently detected when the desired capacity is reached.

input spikes are detected. The AHP of Pi neurons prevents bursting when the input consists of multiple simultaneous spikes. The Pi population acts as an input detector that is independent of the number of spikes that represent the input, as shown in membrane response G in Fig. 4.

The interneuron population Ir also receives excitatory input (with a bi-exponential postsynaptic response with  $E_{rev} = 0$  mV,  $G = 1.2$  nS,  $\tau_{rise} = 0.1$  ms and  $\tau_{fall} = 10$  ms) at theta frequency (H in Fig. 4), at a phase offset (32 ms) that depolarizes the interneurons in synchrony with the expected reactivation phase of the first item that is maintained in the buffer. Input of spikes generated by the Pf pyramidal population is received at synapses with slow bi-exponential timing constants of the postsynaptic response ( $E_{rev} = 0$  mV,  $G = 0.5$  nS,  $\tau_{rise} = 20$  ms and  $\tau_{fall} = 60$  ms). Therefore, depolarization by that postsynaptic potential can combine with input of spikes from the Pi pyramidal cells at synapses with faster bi-exponential response timing ( $E_{rev} = 0$  mV,  $G = 0.5$  nS,  $\tau_{rise} = 10$  ms and  $\tau_{fall} = 60$  ms) to elicit spiking in the population of interneurons (membrane response I in Fig. 4). When input indicates both a buffer filled to capacity and the arrival of afferent input, spiking of the Ir interneurons (limited by an AHP with  $E_{rev} = -90$  mV,  $G = 4$  nS,  $\tau_{rise} = 4$  ms and  $\tau_{fall} = 50$  ms) provides GABAergic inhibitory input to all intrinsically spiking buffer neurons ( $P_{ADP}$  in Fig. 4) through synapses with reversal potential  $E_{rev,Ir} = -90$  mV, conductance amplitude  $G_{Ir} = 40$  nS and bi-exponential time constants  $\tau_{rise,Ir} = 1$  ms and  $\tau_{fall,Ir} = 5$  ms. This replacement inhibition specifically suppresses spikes at the phase interval during which the ADP of the spikes that represent the first item maintained in the buffer could elicit reactivation spikes. As the ADP begins to decline, spiking is no longer possible and the item is removed from the buffer. The buffer can then support the maintenance of the new item, as ADP reactivates the spikes elicited by afferent input as the last pattern of spikes in

the buffered sequence.

In order to achieve complete first item suppression through a short replacement inhibition at the first item reactivation phase, specific conditions must be met: (1) At first item reactivation time,  $t_{fr}$ , the contributions of theta plus ADP begin to elevate membrane potential above the firing threshold. (2) At times  $t \geq t_{fr}$ , the combined contributions of theta modulation plus ADP plus gamma inhibition always lead to membrane potential below the firing threshold. These two conditions are met if the time interval between the previous reactivation time of the first item and  $t_{fr}$  is approximately equal to the time taken to reach peak ADP, and if theta modulation is flat or its contribution increases more slowly than the contribution of ADP decreases after  $t_{fr}$ <sup>5</sup>.

## 2 RESULTS

A buffer mechanism for sequences of spike patterns that is independent of synaptic connectivity is necessary for their encoding in episodic memory. In a realistic setting, the spike patterns that make up a sequence to be encoded in episodic memory may be elicited by input stimuli with intervening time intervals of arbitrary duration. The Hebbian process of STDP depends on pre- and postsynaptic spiking that occurs within a time interval of at most 20 to 40 ms (Levy and Stewart, 1983; Markram *et al.*, 1997; Bi and Poo, 1998). Therefore, a buffer that repeatedly reactivates a time-compressed version of a sequence of spike patterns is ideally suited to meet the requirements for encoding in episodic memory.

Initial simulations illustrated problems with the absence of an item replacement mechanism. Figure 5 shows how distinct input and reactivation modes appear in the persistent spiking buffer and that FIFO replacement is not ac-

---

<sup>5</sup>If the ADP response exhibits a steeper decline then a greater proportion of each theta cycle may be used for item reactivation. A more rapid termination of the effect of an intrinsic response (such as the ADP) may be achieved by providing an opposing current with an onset at the desired time of termination (such as an inhibitory postsynaptic potential).

complished simply by adding new input to a full buffer, as was suggested for item replacement in Jensen *et al.* (1996).

- Figure 5 about here -

### Testing buffer function and the replacement mechanism

A simulation of buffer performance with the proposed first-in-first-out item replacement mechanism is shown in Figure 6. The spiking representations of successively presented items (A-F) were acquired in the buffer and short-term memory was maintained by persistent firing, without synaptic modification. Input spikes (see the afferent spike for item E in Fig. 6c) were presented only once and item representations consisted of different numbers of simultaneous spikes. Figure 6a shows that representations with two to eight spikes were maintained in order by a buffer that used a single interneuron model to achieve competitive inhibition. The inhibition appears as a visible gamma oscillation superimposed on the theta rhythm in Fig. 6c, during the reactivation of item representations. The sequence of reactivation maintained the order, but compressed the time between successive item presentations.

Fig. 6c indicates that the timing of spiking in the model would allow STDP to modify synapses between neurons that are activated by the output of the buffer in order to achieve autoassociative encoding of item representations. The buffer output may also enable episodic encoding with greater STDP time windows (Koene *et al.*, 2003; Koene and Hasselmo, 2005), in which synaptic strengthening by STDP depends on the size of the time interval between spikes (Jensen and Lisman, 1996b; Koene, 2006a). Figures 6b and 6c show the spiking of replacement interneurons (I) and the consequent suppression of the first set of persistent spikes. Replacement inhibition removed the representation of item A as item E appeared, and removed the representation of item B as item F appeared, so that a buffer capacity of four spiking item representations was

achieved. In each case, the spike representation of the new item reactivated to take the last position in the buffered sequence.

- Figure 6 about here -

### **The significance of characteristic model parameters**

We may predict functional changes that result from modifications of specific characteristic parameter values of the buffer model. Transmission modulation of the input to pyramidal cells in the full buffer detector (Pf in Fig. 4) is a critical variable of the proposed mechanism. We predict that such transmission modulation exists in ECII. If it does not, then the alternative approach is to supply phase-specific filtering through strong theta modulation of the pyramidal cell in the full detector. That modulation can take the form of rhythmic excitatory and/or inhibitory input.

Transmission modulation of the recurrent inhibition that is observed as gamma rhythm is not critical, as it merely limits how close together afferent input and the first item reactivation can appear. Without mode-specific modulation, the recurrent gamma inhibition that occurs as a result of pyramidal spikes elicited by afferent input imply that a minimum interval must lie between the afferent input spikes and the first item reactivation spikes (Fig. 7). In the special case of a type of reverse order STM buffer that depends on the phase of afferent input (demonstrated in Fig. 8) proposed transmission modulation of recurrent inhibition may affect buffer function.

- Figure 7 about here -

The buffer works with AHP conductance values between 25 nS and 35 nS. If the AHP is too strong, it suppresses reactivation (especially reactivation in the same theta cycle, as is necessary when new input is received in the STM buffer). If the AHP is too weak then different combinations of ADP and theta modulation are needed for a functioning buffer, otherwise a spike pattern may

appear more than once in a theta cycle, which causes a deterioration of the order and distinctness of items maintained in the buffer. Changing the conductance or the fall time of the AHP can both change the effective strength of the AHP, with consequences as described above.

An ADP rise time of 90 ms to 160 ms results in a working buffer. Our evaluation of the buffer model indicates that there is some room for variations of the intrinsic characteristics. The buffer model does not require extreme fine-tuning of physiological parameters, so that neurons with a range of acceptable characteristic parameter values can participate as buffer neurons in ECII. Buffer function requires precision for phase-locking in the following parameters: (a) The phase at which input is received by the buffer. (b) The phase at which a full buffer is detected. (c) The phase at which replacement inhibition occurs in the buffer. Fortunately, phase specific sensitivity can be learned.

### **Reverse buffering**

The buffer reactivated and maintained a sequence of spikes in the reverse order of their initial presentation when a specific relationship of characteristic parameters was used, as shown in figures 8 and 9. This function is predicted if the rise time constant and amplitude of the ADP response are such that a new input spike does not lead to a reactivation spike within the same theta cycle. If neurons exist that respond in this way then a reverse order persistent spiking buffer provides a mechanism for the repeated presentation of item spikes needed to establish a backward association with spike-timing dependent plasticity. When learning from realistic training input in which the stimuli of one trial are presented once in a specific order, such backward associations are needed in models of goal-directed behavior that rely on converging forward and reverse spread of activity through neurons, each of which represent an item in a sequence of items (such as places or stimuli) encountered (Hasselmo, 2005; Koene and Hasselmo, 2005), or

in models of context dependent retrieval of episodes (Hasselmo and Eichenbaum, 2005).

- Figure 8 about here -

- Figure 9 about here -

### **The effect of the theta frequency and of the strength of competitive inhibition on buffer capacity**

In figure 10, we show that the capacity of the buffer is increased to seven items when we lower the frequency of the theta rhythm that septal inputs are assumed to provide to 5 Hz. By retaining the same strength of the recurrent inhibition in the network, more gamma cycles were nested within the depolarizing reactivation phase interval of the extended theta cycle duration.

- Figure 10 about here -

When instead we manipulate only the conductance parameter for the inhibitory response produced at pyramidal cells due to recurrent input from the “gamma” interneuron network, we show that strengthening that inhibition leads to a smaller capacity of STM (Fig. 11). Stronger gamma inhibition delays the spiking of successive spike patterns maintained in the buffer, which results in a lower observed gamma frequency. Fewer gamma cycles at that frequency fit into the depolarizing reactivation phase interval of the theta rhythm.

- Figure 11 about here -

Conversely, the capacity of STM may be increased if gamma inhibition is weakened. Given a specific theta frequency, the capacity of STM that can be achieved in this way is limited by a critical value for the strength of recurrent gamma inhibition. Below this value, the competitive inhibition that one pattern of pyramidal spikes elicits by activating the gamma interneuron network is insufficient to maintain separation from the following pattern of buffered spikes by a minimum time interval. In figure 12, we show that STM function deteriorates

rates with weak gamma inhibition ( $G_{\text{gamma}} < 2.5$  nS). After a few theta cycles, initially distinct patterns of spikes merge to spike simultaneously. For reliable buffer performance, a greater minimum strength of gamma inhibition is needed when we take into account the influence of noise in biological systems, such as in several of the simulations described in following results.

- Figure 12 about here -

### **The effect of interference between item representations**

We considered the case where the sets of spikes that are consecutively elicited by a sequence of afferent input are not completely distinct. A pyramidal cell of the buffer that has spiked and experiences after-depolarization may spike due to afferent input. When that happens, the after-depolarization response is reset in order to model the resetting of internal calcium concentration of the cell as a consequence of the spiking action. The afferent input therefore determines the new phase of the buffer cycle at which a spike is reactivated, and that spike no longer contributes to the same representation of a buffered item. This is shown for the case of two items with overlapping spiking representations, C and F in Figure 13. When the spiking representation of F entered the buffer, the representation of C was reduced to a smaller subset of spikes (C'). If C is a known item that has been previously encoded in a recurrent network then the reduction of C may be countered by autoassociative retrieval into the buffer (Koene, 2006b). The spike representation and reactivation of the new item F were not affected.

- Figure 13 about here -

If afferent input causes spikes that match the complete representation of a buffered item then that item will reactivate only in the temporal order (buffer position) of the new input. The original temporal position of the item representation that reappeared while buffered is lost and the sequence shifts to fill

the blank location. If the same input is presented multiple times consecutively then buffer content will not appear to change and will contain only one instance of the corresponding item representation. No effect is noticeable if novel input presents the same set of spikes that represent the first item in a buffer that is filled to capacity.

This loss of a previous instance of an item representation that matches new input was simulated in prior work for a delayed non-match to sample task (McGaughy *et al.*, 2005) to show that it may explain specific errors in the observed behavior of rats (McGaughy *et al.*, 2004). In the experiment, rats were trained to sniff consecutively at two different odors (A and B). Following a delay, the rats were given a test odor, after which the task required that the rat dig in one of the original two containers to point out the one with the non-matching odor. Rats with prefrontal cortex lesions, but intact entorhinal cortex displayed a peculiar performance error. If trained rats were presented with odors A and B, then with a test odor matching A, they had no difficulty identifying the separate test container with odor B. When those rats were given a test odor matching the second of the two sample odors (B) then they were confused by the repetition, and were unable to perform the task. They eventually picked a container at random (chance level performance).

Given a buffer capacity of two items, our model predicts that a reduction of buffer content is caused by the presentation of the same stimuli that elicited maintenance of that last (i.e. second) item in the buffer. As explained above, this is predicted for all cases where spiking due to new input matches a spiking representation that is maintained in the buffer. Each buffered item may represent knowledge of an odor and an associated container. When the test phase involves input of B then the replacement mechanism removes A from the full buffer. Only one item (B) remains in the buffer. According to our model, the

rats with prefrontal lesions are left with insufficient information in that case to perform the two comparisons that are expected in the DNMS task.

Two item STM capacity may be unlikely. Alternatively, we may consider a plausible three item buffer capacity, in which the third buffered item represents some interceding event, such as a perception of the switch from sample presentation to the delay and performance parts of the task. We show simulation results for both capacities, two item capacity in Fig. 14a and three item capacity in Fig. 14b. When a buffer limited to two items is assumed, a phase offset of 53 ms is used for the transmission modulation of buffer output into neurons detecting the full buffer state, while the conductance amplitude of the input from those detector neurons to the replacement interneurons is raised to  $G = 1.0$  nS.

- Figure 14 about here -

### **A reliable model of short-term memory deals gracefully with noise**

We evaluated the effect of noise on the function of the STM buffer, when the reactivation of novel patterns of simultaneous spikes relies entirely on persistent firing without synapse dependent retrieval. Noise was added through simulated current clamps of individual neurons driven by a first order autoregressive process (a model for the response to noise that is similar to a random walk) with Poisson distribution, a mean value of 0, amplitude 1 pA and regression parameter 0.5. With this noise, we evaluated the statistical probability of errors in the buffered patterns of spikes by performing 50 simulation runs, each over 5000 ms, presented with six stimuli that were represented by patterns consisting of between 2 and 8 simultaneous spikes with a total of 28 active neurons. Of the 50 runs, 27 simulation runs produced no errors. The mean error quantified as all missing or extra spikes at the end of a simulation run was 1.22 spikes with a standard deviation of 1.8 (a bit error rate of 0.044). The first item pattern presented to the buffer contained errors in 15 of the 23 runs that exhibited errors

due to noise. In only 2 of the simulation runs did more than one spike pattern contain errors. In both of those runs, the number of patterns involved was 2, and in both cases the first item pattern presented to the buffer was one of those. Never was an entire spike pattern lost to noise.

During some simulation runs, individual spikes of the first pattern in the STM buffer stopped reactivating if noise delayed reactivation sufficiently so that the competitive recurrent inhibition caused by the remaining spikes suppressed reactivation of the delayed spike until its ADP began to fall. In effect, the spike was removed from the buffer in the same manner as items are removed by the replacement mechanism (Fig. 15). A similar error appears occasionally in items other than the first, if reactivation in the same theta cycle as the presentation of afferent input fails.

- Figure 15 about here -

When noise produces a delay in the reactivation of individual spikes, delayed spikes may end up in a separate gamma cycle, effectively adding another item in the buffer that is then sustained in that order (Fig. 16). For novel items, encoding with such noise effects may separate a single item representation (normally stored through STDP by the strengthening of autoassociative synaptic connections) into multiple parts that are subsequently stored as an episode.

- Figure 16 about here -

In general, the first item in the STM buffer is more susceptible to noise induced errors than the following items that are flanked by gamma inhibition and for which reactivation is driven by combinations of depolarization by theta modulation and ADP that significantly exceed the threshold potential. The membrane potentials of those items exceed the threshold potential before reactivation of spiking, as their spiking is actively delayed by recurrent inhibition. It is notable that even in the presence of relatively strong noise (with values

up to  $\pm 10$  pA), several of the spikes in each item pattern tend to survive the difficult insertion into the buffer and continue to reactivate in the correct order (Fig. 17a). As even stronger noise is added (values that reach  $\pm 60$  to  $\pm 70$  pA), the duration of item maintenance in the STM buffer is limited by the drop-out of spikes (Fig. 17b).

- Figure 17 about here -

### 3 DISCUSSION

We hypothesize that persistent firing characteristics of pyramidal cells in ECH can provide a reliable short-term buffer for tasks in which encoding of autoassociative and episodic memory depends on the rapid acquisition and maintenance of novel item representations. We propose an explicit mechanism for the first-in-first-out ordered replacement of items in a buffer filled to capacity, and we show that the buffer mechanism can be specified with a range of parameter values and modifications of its specific function.

As in previous simulations by Lisman and Idiart (1995) and by Jensen *et al.* (1996), our results show (Fig. 6) that the buffer function is achieved without dependence on synaptic modification. Patterns of simultaneous spikes are acquired from a single presentation of input and maintained by persistent firing, regardless of the number of spikes that represent an individual item. The individual items are maintained in their order of presentation, separated from each other by competitive inhibition within a time-compressed sequence of spike patterns. We demonstrated the need for an explicit mechanism that can remove the oldest item in the buffer to make room for a new item when novel input appears more rapidly than buffered items are extinguished by other causes, such as noise and slow after-hyperpolarization of the pyramidal cells.

In the simulations by Jensen *et al.* (1996), new items were presented after

the end of the repetition of the items in the buffer, separated by a time interval similar to the duration of one gamma cycle. The input phase in the present model has a similar temporal separation from the last spike during the preceding reactivation of buffer content. Despite this similarity in the input protocol, the addition of new input to a full buffer does not result in the correct FIFO replacement of the oldest item when no additional mechanism is provided for that purpose. A replacement mechanism represented by two pyramidal cells and one interneuron is able to perform the first-in-first-out item replacement for buffered item representations with two to eight spikes. When each node in the model replacement mechanism is expressed as an actual population of neurons, the range of pattern sizes that can be dealt with may be multiplied accordingly.

Three critical parameters of the STM model involve timing that is locked to specific phases of theta rhythm: (1) Input to the buffer must be filtered to appear at a phase that does not interfere with the reactivation of items in the buffer and that allows the ADP to reactivate new spikes near the end of the same theta cycle. (2) The phase offset of transmission modulation of input to those pyramidal cells that detect a full buffer state determines the working capacity of the buffer. That capacity can be less than the maximum capacity made possible by characteristic theta and gamma frequencies<sup>6</sup>. (3) Replacement inhibition must extinguish the reactivation of spikes representing the first item maintained in the buffer, which occurs if the onset of inhibition is at a specific phase of the buffer cycle.

There is some room for biological variability in the parameters of the model that depend on specifics of neurophysiology. The strength of after-hyperpolarization

---

<sup>6</sup>For example, compare the five item capacity of buffer function in Fig 5 and the four item capacity of buffer function in Fig 6. The two simulations have all parameter values in common (implying the same theoretical maximum capacity) except the size of the phase offset of the transmission modulation of input for the detection of a full buffer, which causes different working capacity.

and the timing of the after-depolarization of buffer pyramidal cells may vary within a range of acceptable values. While transmission modulation is helpful, it is not essential for the rapid alternation of afferent input and reactivation phases in the buffer, and may also be replaced in an alternative implementation of the model of the replacement mechanism. The phase sensitivity of neurons that act as the full buffer detector may instead be accomplished by assuring that spiking depends on rhythmic depolarization at theta frequency.

Buffering items in the reverse order of their presentation is a useful modification of the buffer function and was achieved in two ways through minor changes of model parameters. Modification of parameters that determine the frequency of theta rhythm and the strength of gamma inhibition directly affect the maximum buffer capacity, and a minimum gamma inhibition is necessary to ensure buffer function that maintains separate items. Beyond this absolute functional minimum strength of competitive inhibition, stronger inhibition and therefore greater intervals of item separation may be desirable for a different reason. Item separation with very small intervals may be problematic when the output of the buffer is used to elicit autoassociative encoding by STDP with a realistic time window for effective synaptic strengthening in a network with recurrent connections. The STDP may lead to unwanted episodic encoding when the time interval between the spike patterns of consecutive items is too small. This reason for a greater minimum strength of gamma inhibition in the model and the consequent realistic nesting of  $4 \pm 1$  item reactivation phases per theta cycle are examined in greater detail elsewhere (Koene, 2006b). The combination of common theta and gamma frequencies lead to buffer capacities in the observed range of  $4 \pm 1$  items (Cowan, 2001).

Our simulation results predict that the temporal context of items held in short-term memory may be forgotten if an item is presented more than once.

This prediction depends critically on two presuppositions of the model, namely (1) the intrinsic nature of item maintenance due to after-depolarization and (2) the explicit replacement mechanism. It may explain specific errors that were observed in rats with prefrontal cortex lesions, but intact entorhinal cortical function, performing a delayed non-match to sample task (McGaughy *et al.*, 2005). A possible solution to the problem when multiple instances of the same input are presented to the buffer with few intervening items (i.e. within buffer capacity) is explored in prior (Koene, 2001) work and in a paper that is currently in preparation (Koene, 2006c). The solution presented there involves the recruitment of spontaneous spikes within the buffer as part of item representations, which may therefore constitute different (though overlapping) sets of spikes for each input presentation.

We found that buffer performance deteriorates gracefully as the noise that affects the timing of buffer spikes increases. This deterioration takes place in two stages: (1) Low levels of noise reduce the number of spikes that represent each item that is maintained in the buffer. (2) High levels of noise also affect the duration of persistent firing in a nondeterministic manner. Consequently, items that are represented by a large number of spikes may be maintained in STM for a longer average period of time than those represented by a small number of spikes. The maintenance of a specific item becomes improbable beyond a duration that is determined by the signal to noise ratio. This feature resembles the assumptions that underlie a theory for the representation of temporal context proposed by Howard and Kahana (2001). A buffer with these characteristics is a useful short-term memory for novel items that must be encoded autoassociatively. When the buffer function is combined with autoassociative retrieval, it is a reliable short-term memory for sequences that are encoded in episodic memory (Koene, 2006a).

**Improved modeling of realistic response mechanisms affects functional requirements**

The neurophysiology modeled here better represents realistic response mechanisms than previous models of persistent spiking buffers that are based on intrinsic mechanisms. Integrate-and-fire neuron dynamics are used in the construction of the present model of short-term memory. These dynamics include a neuronal membrane capacitance that affects the time-course of membrane potential when positively or negatively influenced by integrated synaptic responses or intrinsic mechanisms. Capacitance and the leak current were not included explicitly in the buffer models of Lisman and Idiart (1995) and of Jensen *et al.* (1996), and in prior work by Koene (2006b). This distinction can lead to significantly different requirements that deal with the dynamics of a persistent spiking STM. The capacitance and leak current determine the characteristics of a gradual return of membrane potential to the resting potential. They temporally constrain the cumulative effect of changes in the membrane potential caused by postsynaptic responses and intrinsic mechanisms that are initiated at different times.

The proposed method of item replacement requires that the first item maintained in STM reactivates at the earliest phase at which the combination of depolarizing theta modulation and ADP reaches threshold, and that the duration of a theta period is approximately equal to the rise time of the ADP. The first requirement is guaranteed after a few cycles of item reactivation, since the theta response assures that item reactivation shifts to its earliest possible phase.

The functional requirements of item replacement in the buffer model are also changed by the increased realism of our model. In contrast with the present model, Jensen *et al.* (1996) assumed one homogeneous population of interneurons that act as a single network-wide inhibitor in response to an action potential

of any pyramidal neuron. They postulate that this one mechanism of network inhibition is responsible both for the observed gamma oscillations, as well as the suppression of the oldest item in a STM buffer when novel input causes pyramidal spiking after the last cycle of sequence reactivation. Since the delay of spike propagation and the response timing of a single mechanism are fixed, this means that spiking for novel input must occur no earlier than one gamma interval prior to the onset of the next cycle of sequence reactivation. As we showed, such timing does not allow the novel item to reactivate in the same theta cycle, which leads either to the inability to maintain a representation of the novel item or to reverse order buffering if the time constant of rising ADP is sufficiently great. Therefore, we present the item replacement mechanism that involves a second subset of the interneurons in ECII. We predict that those interneurons activate irregularly and less frequently, namely in those specific cases when STM capacity has been reached and novel input must be acquired in STM.

### **Neuroanatomical support for phase specific inhibition in entorhinal cortex as required by the item replacement mechanism**

Many different types of interneuron have been identified in the medial temporal lobes (Freund and Buzsaki, 1996; Gulyás *et al.*, 1999). Two of these types of interneuron are believed to be involved in the nested theta and gamma rhythms in the hippocampal system (White *et al.*, 2000). Recent observations have shown that some groups of specific interneuron types (such as CB1-expressing interneurons) predominantly spike irregularly. We predict that such interneurons may be preferentially active at specific phases of the theta cycle and the specific phase can differ as needed. We presuppose this differentiation between populations of interneurons, which play different functional roles in the entorhinal cortex. One population of interneurons may provide the inhibitory feedback that is detected

as the gamma rhythm, while another population of interneurons may conditionally provide inhibition that suppresses first item activation in a persistent spiking buffer in ECII.

**The repeated appearance of spikes caused by afferent input can lead to a reduction of buffer content**

Our default parameter values specify a theta cycle duration and strength of gamma inhibition with which the maximum achievable buffer capacity is to sustain the firing of five items (detecting “full” state at a phase offset of 103 ms). When item replacement occurred in a buffer filled to maximum capacity ( $N_{max}$ ), we observed a toggling of the number of items maintained in the buffer, between  $N_{max}$  and  $N_{max} - 1$ . In the case where  $N_{max} = 5$ , the buffer can accept and maintain a fifth item when it contains only four items. If the buffer is already full then another input causes replacement inhibition that suppresses the first item, but the new item presented by afferent input cannot reactivate in the buffer during that theta cycle, since the item reactivation phases for items 2 to  $N_{max}$  are still occupied. The buffer maintains the remaining four spike patterns until another input arrives, which is then maintained in the fifth reactivation phase. Maintaining  $N_{max}$  items can therefore depend on a specific input protocol, which requires two presentations of novel input once the buffer is full. Robust capacity with no special input protocol requirements and our proposed default parameter values is therefore  $N = 4$  items (achieved by detecting “full” state at a phase offset of 84 ms). At that capacity, the depolarizing phase of theta modulation in buffer pyramidal cells extends sufficiently beyond the Nth item reactivation phase to enable a new item representation to reactivate in the same theta cycle.

**Noisy short-term memory is sufficiently reliable to support encoding by spike-timing dependent potentiation**

In the presence of noise, we predict that the maintenance of ordered patterns of spikes in the buffer deteriorates gracefully in the sense that the buffer output provided by cycles of pattern reactivation (Fig. 17b) can enable encoding of an episodic representation in a recurrent network through STDP. This graceful deterioration is marked by noise errors that are predominantly categorized as the loss (or drop-out) of spikes in representative spike patterns, rather than the splitting of patterns or changes in the order of maintained spikes. The latter type of errors would be more problematic, since they could lead to false associations through synaptic modification by STDP. Specific reasons for the predominance of drop-out errors are: (1) Greater sensitivity of the buffer to the timing of the reactivation of the first item, since the combination of depolarization by theta modulation and peak after-depolarization is just sufficient for reactivation at the first item phase. (2) The overall tendency that the earliest spikes within a noisy pattern of near-simultaneous spikes lead to competitive suppression durable enough to prevent spiking of the suppressed neurons, especially during the reactivation phase interval of the first item. (3) Errors in later item spike patterns that are also maintained in the buffer are more able to produce problematic shifts instead of drop-out, but are less likely to occur, due to stronger depolarization at later phases of theta modulation and a phase of the spike onset that is constrained by preceding gamma inhibition.

When item separation deteriorates, as shown for the case of insufficient gamma inhibition in figure 12, the merged spiking output of the buffer no longer induces episodic encoding. Target regions with recurrent synapses modified by spike-timing dependent plasticity may then erroneously encode a single autoassociative representation for the merged patterns of spikes.

The noisy maintenance of three to four items in Fig. 17b, in a first-in-first-out ordered manner, demonstrates that the buffer provides many theta cycles in which STDP may encode the episodic relationship between consecutive novel items. Deterioration due to noise may be countered in the case when the buffer maintains a sequence of known (previously encoded) autoassociative spike patterns. This is achieved by synaptic modification in sparse recurrent fibres within ECII and by error correction (pattern completion) through the retrieval of stored autoassociative spike patterns in ECIII, as presented in a separate paper (Koene, 2006a).

The signal to noise ratio of the system may itself be a significant characteristic of the mechanism. For instance, a STM buffer may not need to develop a phase-locked mechanism for item replacement in the presence of strong noise. Such a replacement mechanism would only be needed if the rate at which item replacement by new input is desired is faster than the rate at which all spikes of the oldest item in the buffer are extinguished by the effects of noise. Unfortunately, strong noise places greater limitations on the maximum duration of item maintenance in STM. That limitation may be countered by using a larger number of spikes to represent each item, but then an explicit replacement mechanism, as proposed in this study, may again be needed.

## Acknowledgment

The CATACOMB simulations described here and information about the CATACOMB environment created and maintained by Robert C. Cannon are available on our Computational Neurophysiology web site at <http://askja.bu.edu>.

Supported by NIH R01 grants DA16454, MH60013 and MH61492 to Michael Hasselmo and by Conte Center Grant MH60450.

Address correspondence to R.A. Koene, Center for Memory and Brain, De-

partment of Psychology and Program in Neuroscience, Boston University, 64  
Cummington Street, Boston, MA 02215, U.S.A. Email: randalk@bu.edu.

## References

- Alonso A, Gaztelu J, Bruno Jr. W, Garcia-Austt E (1987). Cross-correlation analysis of septohippocampal neurons during theta-rhythm. *Brain Research* 413:135–146.
- Bi G, Poo M (1998). Synaptic modifications in cultured hippocampal neurons: Dependence on spike timing, synaptic strength, and postsynaptic cell type. *Journal of Neuroscience* 18(24):10464–10472.
- Bliss T, Collingridge G (1993). A synaptic model of memory: Long-term potentiation in the hippocampus. *Nature* 361:31–39.
- Bliss T, Lømo T (1973). Long-lasting potentiation of synaptic transmission in the dentate area of the anaesthetized rabbit following stimulation of the perforant path. *Journal of Physiology* 232:331–356.
- Bragin A, Jando G, Nadasdy Z, Hetke J (1995). Gamma (40-100 Hz) oscillation in the hippocampus of the behaving rat. *Journal of Neuroscience* 15:47–60.
- Brazhnik E, Fox S (1999). Action potentials and relations to the theta rhythm of septohippocampal neurons in vivo. *Experimental Brain Research* 127:244–258.
- Buzsáki G, Leung L, Vanderwolf C (1983). Cellular bases of hippocampal EEG in the behaving rat. *Brain Research* 287:139–171.
- Cannon R, Hasselmo M, Koene R (2003). From biophysics to behaviour: Catacomb2 and the design of biologically plausible models for spatial navigation. *Neuroinformatics* 1:1:3–42.

- Cowan N (2001). The magical number 4 in short-term memory: A reconsideration of mental storage capacity. *Behavioural and Brain Sciences* 24:1:1.
- Egorov A, Hamam B, Franssen E, Hasselmo M, Alonso A (2002). Graded persistent activity in entorhinal cortex neurons. *Nature* 420(6912):173–178.
- Fox S (1989). Membrane potential and impedance changes in hippocampal pyramidal cells during theta rhythm. *Experimental Brain Research* 77:283–294.
- Fox S, Wolfson S, Ranck J (1986). Hippocampal theta rhythm and the firing of neurons in walking and urethane anesthetized rats. *Experimental Brain Research* 62:495–508.
- Freund T, Buzsáki G (1996). Interneurons of the hippocampus. *Hippocampus* 6:347–470.
- Gulyás A, Megias M, Emri Z, Freund T (1999). Total number and ratio of excitatory and inhibitory synapses converging onto single interneurons of different types in the CA1 area of the rat hippocampus. *Journal of Neuroscience* 19(22):10082–10097.
- Hasselmo M (2005). A model of prefrontal cortical mechanisms for goal directed behavior. *Journal of Cognitive Neuroscience* In press.
- Hasselmo M, Bodelon C, Wyble B (2002a). A proposed function for hippocampal theta rhythm: Separate phases of encoding and retrieval enhance reversal of prior learning. *Neural Computation* 14(4):793–817.
- Hasselmo M, Cannon R, Koene R (2002b). A simulation of parahippocampal and hippocampal structures guiding spatial navigation of a virtual rat in a virtual environment: A functional framework for theta theory. In *The Parahip-*

- poampal Region: Organization and Role of Cognitive Functions* (Witter M, Wouterlood F, eds.), pages 139–161. Oxford: Oxford University Press.
- Hasselmo M, Eichenbaum H (2005). Hippocampal mechanisms for the context-dependent retrieval of episodes. *Neural Networks* 18(9):1172–1190.
- Hebb D (1949). *The Organization of Behavior*. New York: Wiley.
- Howard M, Kahana M (2001). A distributed representation of temporal context. *Journal of Mathematical Psychology* IDEALfirst:1388.
- Jensen O, Idiart M, Lisman J (1996). Physiologically realistic formation of autoassociative memory in networks with theta/gamma oscillations: Role of fast NMDA channels. *Learning & Memory* 3:243–256.
- Jensen O, Lisman J (1996a). Novel lists of  $7 \pm 2$  known items can be reliably stored in an oscillatory short-term memory network: Interaction with long-term memory. *Learning & Memory* 3:257–263.
- Jensen O, Lisman J (1996b). Theta/gamma networks with slow NMDA channels learn sequences and encode episodic memory: Role of NMDA channels in recall. *Learning & Memory* 3:264–278.
- Klink R, Alonso A (1997a). Morphological characteristics of layer ii projection neurons in the rat medial entorhinal cortex. *Hippocampus* 7:571–583.
- Klink R, Alonso A (1997b). Muscarinic modulation of the oscillatory and repetitive firing properties of entorhinal cortex layer ii neurons. *Journal of Neurophysiology* 77(4):1813–1828.
- Koene R (2001). *Functional requirements determine relevant ingredients to model for on-line acquisition of context dependent memory*. Ph.D. thesis, Department of Psychology, McGill University, Montreal, Canada.

- Koene R (2006a). Concurrent encoding and retrieval is based on rhythmic modulation of context dependent memory in dentate gyrus and regions CA3 and short-term memory in entorhinal layer II. Submitted.
- Koene R (2006b). Short-term memory based on intrinsic neuronal dynamics during on-line acquisition of context dependent memory. Submitted.
- Koene R (2006c). Spiking activity in dentate gyrus enables recruitment of coactivating neurons to encode sequences without interference. In preparation.
- Koene R, Gorchetchnikov A, Cannon R, Hasselmo M (2003). Modeling goal-directed spatial navigation in the rat based on physiological data from the hippocampal formation. *Neural Networks* 16(5-6):577–584.
- Koene R, Hasselmo M (2005). An integrate and fire model of prefrontal cortex neuronal activity during performance of goal-directed decision making. *Cerebral Cortex* 15(12):1964–1981. Advanced Access published on April 27, 2005.
- Levy W, Stewart D (1983). Temporal contiguity requirements for long-term associative potentiation/depression in the hippocampus. *Neuroscience* 8(4):791–797.
- Lisman J, Idiart M (1995). Storage of  $7 \pm 2$  short-term memories in oscillatory subcycles. *Science* 267:1512–1515.
- Markram H, Lübke J, Frotscher M, Sakmann B (1997). Regulation of synaptic efficacy by coincidence of postsynaptic apss and epsps. *Science* 225:213–215.
- McGaughy J, Koene R, Eichenbaum H, Hasselmo M (2004). Effects of cholinergic deafferentation of prefrontal cortex on working memory: A convergence of behavioral and modeling results. In *Proceedings of the 2004 Annual Meeting of the Society for Neuroscience*. San Diego, CA.

- McGaughy J, Koene R, Eichenbaum H, Hasselmo M (2005). Cholinergic deafferentation of the entorhinal cortex in rats impairs encoding of novel but not familiar stimuli in a delayed nonmatch-to-sample task. *Journal of Neuroscience* 25(44):10273–10281.
- Skaggs W, McNaughton B, Wilson M, Barnes C (1996). Theta phase precession in hippocampal neuronal populations and the compression of temporal sequences. *Hippocampus* 6:149–172.
- Stewart M, Fox S (1990). Do septal neurons pace the hippocampal theta rhythm? *Neuron* 13:163–168.
- Wallenstein G, Hasselmo M (1997). Bursting and oscillations in a biophysical model of hippocampal region CA3: implications for associative memory and epileptiform activity. In *Computational Neuroscience* (Bower J, ed.). New York: Plenum.
- White J, Banks M, Pearce R, Kopell N (2000). Networks of interneurons with fast and slow  $\gamma$ -aminobutyric acid type a ( $gaba_a$ ) kinetics provide substrate for mixed gamma-theta rhythm. *Proceedings of the National Academy of Sciences* 97(14):8128–8133.
- Wyble B, Hyman J, Rossi C, Hasselmo M (2004). Analysis of theta power in hippocampal EEG during bar pressing and running behavior in rats during distinct behavioral contexts. *Hippocampus* 14(5):662–674.

## Legends

Figure 1: Detecting the need for item replacement due to activity at specific phases of theta modulation in a short-term memory buffer based on persistent spiking. The buffer shown here is designed to hold a maximum of two items. Spikes at phases (c) and (a) represent items maintained in the buffer. The spike at (b) represents input that inserts a new item into the buffer.

Figure 2: Simulated membrane potential of cells in entorhinal cortex layer II that exhibit cholinergic activation of sustained spiking activity due to an intrinsic afterdepolarization (ADP). Control condition, Low ACh: Spiking activity is elicited in neurons by a 400 ms current injection. The activity ends when current injection is terminated. High ACh: Spiking activity during current injection causes activation of a subsequent afterdepolarization due to the activation of muscarinic cholinergic receptors. Each spike is followed by a brief afterhyperpolarization, then an afterdepolarization that can lead to another spike. High ACh plus theta modulation: Spiking at regular intervals that is synchronized with theta rhythm results when the depolarizing phase of cholinergic theta modulation combines with ADP to elevate membrane potential to the spiking threshold. Intrinsic currents cause this sustained spiking, which does not depend on recurrent excitatory synaptic connections.

Figure 3: The buffer model operates in alternating functional phase intervals: 1. During a reactivation phase interval (bottom, dashed lines), modulation at theta frequency depolarizes pyramidal cells and after-depolarization causes the reactivation of buffered spikes (A and B). The plots of recurrent and afferent transmission modulation (top) show that conductance through afferent input synapses is reduced during the reactivation phase, while the conductance of

recurrent gamma inhibition is strong. That insures that reactivated spikes representing different items in the buffer are separated by competitive inhibition (highlighted in box on C response). 2. During an input phase interval (bottom, solid lines), modulation at theta frequency hyperpolarizes pyramidal cells, so that intrinsic spiking is inhibited. The plots of recurrent and afferent transmission modulation (top) show that conductance of recurrent gamma inhibition is reduced, while the conductance through afferent input synapses is strong. That enables afferent input to elicit new spikes in the buffer neurons (first spike on B).

Figure 4: The input stimuli and pyramidal cell and interneuron population responses of the proposed first-in-first-out item replacement mechanism in the short-term buffer. Two pyramidal cell populations in entorhinal cortex layer II (ECII), represented here by two single neurons, act as detectors of the full buffer state (Pf) and of afferent input to the buffer (Pi). The membrane potential of pyramidal cells Pf experience modulation at theta rhythm by septal input (A) in synchrony with the pyramidal cells that rhythmically reactivate item spikes due to their intrinsic afterdepolarization currents. Transmission modulation (B) of output connections from the buffer cells to Pf cells (indicated at schematic node Tm) at the same theta frequency has a phase offset so that buffer output spikes (shown in C) in the fourth buffered item phase of the reactivation interval are strongly transmitted to the Pf cell population. At the depolarized phase of theta modulation, one to eight such simultaneous inputs cause a Pf cell to spike (D), acting as a full buffer detector. Similarly, the combination of one to twenty simultaneous afferent inputs (E) with rhythmic septal input (F) causes a cell in the Pi subset of pyramidal cells in ECII to spike (G), which acts as an input detector. Septal input at theta rhythm (H) and output spikes of Pf (full buffer detection) and Pi (input detection) pyramidal cells combine to cause

simultaneous spiking (I) of a population of interneurons (here indicated by a single interneuron Ir) that exert replacement inhibition at buffer pyramidal cells  $P_{ADP}$  through recurrent fibres. The phase of septal input insures that replacement inhibition spikes suppress reactivation of the first item in the short-term buffer. The full buffer response (D) exhibits three spurious detection spikes on theta cycles immediately following the first, second and third input stimuli (E), as new item reactivation has yet to shift to earlier phases of the theta cycle (as shown by dotted circles in C). The reponse (I) of the replacement interneurons (Ir) shows that two spikes elicit replacement inhibition when the fifth and sixth input stimuli appear (in E).

Figure 5: A simulation that shows the performance of a buffer with a maximum capacity of five items and no item replacement mechanism, as a sequence of six spike patterns (A-F) is elicited by afferent input that appears at intervals of 750 ms. The items are represented by patterns consisting of different numbers of simultaneous spikes. New items appear more rapidly than buffered items would terminate due to the slow after-hyperpolarization that is included in the model. Items A to E are maintained in the order of their appearance, but the depolarizing phase of theta modulation ends before the spiking representation of item F can be reactivated in the buffer. Without replacing the oldest item in the buffer, the sixth item does not interfere, but is not maintained in the simulation of short-term memory either.

Figure 6: A simulation that shows buffer performance and first-in-first-out item replacement with a short-term memory model that has a four item capacity, as a sequence of six spike patterns (A-F) is elicited by afferent input that appears at intervals of 750 ms. (a) Each item is represented by a different number of

simultaneous spikes (from A to F: 5, 2, 8, 4, 3 and 7 spikes), each of which is shown as a short vertical line in the spike plot. Each pattern of spikes is acquired by the buffer and the spikes are reactivated simultaneously, with visible phase offsets between consecutive patterns in a buffered sequence. When the fifth pattern of spikes (E) appears, the pattern representing A does not reactivate. When the sixth pattern (F) appears, B is no longer maintained. (b) Plots of the membrane potential of the first spiking neuron in each item representation (A-F) show regular modulation in each theta cycle. The membrane potential plotted in I shows spikes of the interneuron population that provides replacement inhibition when new spikes appear in a full buffer due to afferent input. (c) At a greater temporal resolution, plots of membrane potential show the functional significance of the timing of the spikes in the buffer. Reactivated spikes of consecutive items maintained in the buffer fall within a time interval small enough so that output from the buffer to a neuronal network with recurrent connections can enable synaptic modification by spike-timing dependent plasticity that encodes episodic relationships between patterns of spikes. Recurrent gamma inhibition maintains the separation and therefore the order of reactivated patterns of spikes. The time interval of the separation is on the order of the cycle period of observed gamma rhythm. When interneurons I spike, replacement inhibition hyperpolarizes all intrinsically spiking pyramidal cells in the buffer. Without this hyperpolarization, the reactivation of spikes that represent the first item in the buffer occurs at the peak of the neuronal after-depolarization response. When hyperpolarized during replacement inhibition, the after-depolarization begins to decay. The spikes representing A no longer reactivate. The buffer then maintains representations of items B, C, D and E.

Figure 7: Simulated membrane potential of two pyramidal cells in entorhinal cortex layer II, in the absence of proposed theta modulation of recurrent “gamma” inhibition. Neuron A spikes rhythmically as a member of the first pattern of spikes maintained in short-term memory. When a second pattern of spikes is introduced to the buffer, afferent input causes a spike in neuron B. Without transmission modulation, this spiking elicits interneuron activity that produces inhibition of the pyramidal cells through recurrent fibres. If spikes due to afferent input occur in an early phase of the theta cycle, and if the duration of recurrent inhibition is sufficiently brief then the reactivation of spikes in the first buffered item is not suppressed.

Figure 8: A simulated reverse order buffer, in which the reversal of the order of item presentation is a consequence of the late phase of afferent input to the buffer. (a) Plots of the membrane potential of one of the spiking neurons in the buffered representations of each item (A-F) show that new spikes appear at a short time interval before the reactivation of spikes maintained in the buffer. The spikes representing buffered items reactivate in the reverse order of their presentation to the buffer. Item A drops out of the buffer a few theta cycles after item F appears. This shows that first-in-first-out item replacement is achieved without an explicit replacement mechanism, as the spikes representing A are shifted beyond the depolarizing phase of the rhythmic membrane modulation at theta frequency. (b) When the phase of afferent input precedes the reactivation phase of the first item in the buffer with only a short time interval, the after-depolarization (ADP) of the neurons that spike as novel input is received is unable to elicit reactivation within the same theta cycle. If the rise time of the ADP is slightly greater than the duration of a theta cycle then the neurons that spike for B will have a greater depolarization than those that spike for A

at the onset of the next period of rhythmic depolarization. In that theta cycle, B therefore reactivates before A. (c) This reversed order of reactivation is then maintained in the buffer for all patterns of simultaneous spikes that represent items A to F.

Figure 9: A simulated reverse order buffer, in which the reversal of the order of item presentation is a consequence of the time constants used for the model after-depolarization (ADP) response. Membrane potential is plotted for one neuron involved in the spiking representation of each item A to E. A slow rise of the ADP means that spikes representing E, caused by afferent input, do not reactivate within the same theta cycle. A rising ADP is maintained until spiking is possible during the next theta cycle, at which time the replacement mechanism suppresses reactivation of spikes representing item A. As the ADP is still rising, the neurons of E spike before the remaining reactivated spikes. A reverse order of reactivation is then maintained in the buffer for the patterns of spikes that represent items B to E.

Figure 10: Simulated patterns of spikes for seven items (A to G) maintained in a STM buffer with a longer theta frequency (5 Hz). The time span of each theta cycle is 200 ms, and each cycle includes a phase of pyramidal depolarization of greater duration than the depolarized phase in a buffer with 8 Hz theta rhythm. The strength of gamma inhibition was not modified, so that the maximum number of spike pattern that can be reactivated in the depolarized phase of theta rhythm and reliably separated by gamma intervals is increased. This gives the buffer the robust capacity to maintain seven items, plotted as different numbers of simultaneous spikes for items A to G.

Figure 11: Simulated patterns of spikes in a STM buffer with capacity limited by greater strength of gamma inhibition ( $G_{\text{gamma}} = 480$  nS). Six patterns of simultaneous spikes representing items A to F are presented as input to the buffer. A sequence of three of those patterns of spikes can be sustained in the order of presentation by persistent firing.

Figure 12: The membrane potential of four pyramidal buffer neurons, of which pairs spike as members of two separate patterns that represent items A and B. The separation is maintained for five theta cycles, after which all four spikes are reactivated nearly simultaneously, in effect merging the buffered representations of A and B. The loss of separation occurs due to insufficient strength of recurrent gamma inhibition.

Figure 13: Spikes of a short term buffer simulation with six item representations (A-F), of which two (C and F) share a subset of spikes. Spikes labelled I show when the interneurons of the replacement mechanism spike to cause suppression of the first item in the buffer. The spike representation of item F includes five novel spikes and two spikes that previously contributed to the representation of item C. As item F appears, the reactivation of spikes representing B is extinguished and the set of spikes that are reactivated in ensuing theta cycles to represent C is reduced to six spikes (labelled C'). Novel and overlap portions of the spike representation of F reactivate in the proper order, as the most recent and therefore the last item maintained in the buffer.

Figure 14: Spikes of the replacement interneuron and item representations A, B and C. (a) In a buffer with two item capacity, sample odors A and B cause afferent input that elicits representative spikes, which are maintained in a buffer

model of entorhinal cortex layer II. A test odor that matches B is then presented. The afferent input causes replacement interneuron spiking in the full buffer, so that the representation of odor A is removed from the buffer. Only a spike representation of odor B is maintained. (b) In a buffer with three item capacity, a third spike representation is elicited by other stimuli, preceding the delayed presentation of the test odor. Once the test odor is presented, the representation of odor A is removed and only the representation of odor B is maintained.

Figure 15: The drop-out of individual spikes during the presentation of novel input to the buffer in the presence of noise that affects neuronal membrane potentials. (a) The spikes of five pyramidal buffer cells that fire in response to afferent input at  $t=125$  ms are plotted. Spiking in neurons  $A_2$  to  $A_5$  is reactivated rhythmically with minor timing variations due to noise. However, because of the noise the initial spike in neuron  $A_1$  is not reactivated so that this neuron drops out of the pattern of spiking neurons that represents item A. (b) A plot of membrane potentials of the pyramidal cells shows that a momentary reduction of the membrane potential of neuron  $A_1$  during the depolarizing phase of theta modulation delayed its elevation by peak after-depolarization to the threshold potential. The spikes of  $A_2$  to  $A_5$  caused competitive inhibition through the recurrent fibres of the “gamma” interneuron network, further suppressing the membrane potential of  $A_1$ . Following this suppression, the decaying after-depolarization of  $A_1$  could not reach the spiking threshold. (c) A plot of the simulated autoregressive noise, which decreased the membrane potential of  $A_1$  at a critical phase of the theta cycle and thereby effectively removed that neuron from the buffered representation of item A.

Figure 16: Plots of the spike patterns that represent buffered items A to D

show that spiking that is delayed by noise, but does not cause spike drop-out can establish separately sustained spiking. The spikes denoted by A' effectively split the original spike pattern representing item A into two consecutive spike patterns. The split may also affect the perceived capacity of the STM buffer, since the earlier spike pattern representing item A is replaced when afferent spikes appear that represent item D.

Figure 17: Plots of the spike patterns that represent buffered items A to F in the presence of strong noise. (a) Strong noise can significantly reduce the number of spikes that represent a buffered item. Between two and eight simultaneous spikes were elicited as items A to F were presented to the buffer by afferent input. Noisy currents affect the membrane potential of pyramidal buffer cells, so that only a subset of each initial spike pattern successfully reactivated due to the after-depolarization response. The buffer capacity was set to four items, but noise affected detection of the full buffer state during the theta cycle in which item E was introduced. The buffer therefore maintained reduced representations of items A to E in order until item replacement removed item A. Consequently, the reactivated spike representation of item F merged with the spike pattern for E. (b) As the signal to noise ratio was decreased further, the noise also limited the perceived duration of short-term memory. Failed spike reactivation terminated the maintenance of each item representation before the presentation of a fifth item to a full buffer could trigger the item replacement mechanism (which otherwise should have terminated the bottom spike in A first). Despite this, the simulation achieved a noisy first-in-first-out buffering of sequences of three to four representations of the items A to F in which order was largely undistorted.



## Figures

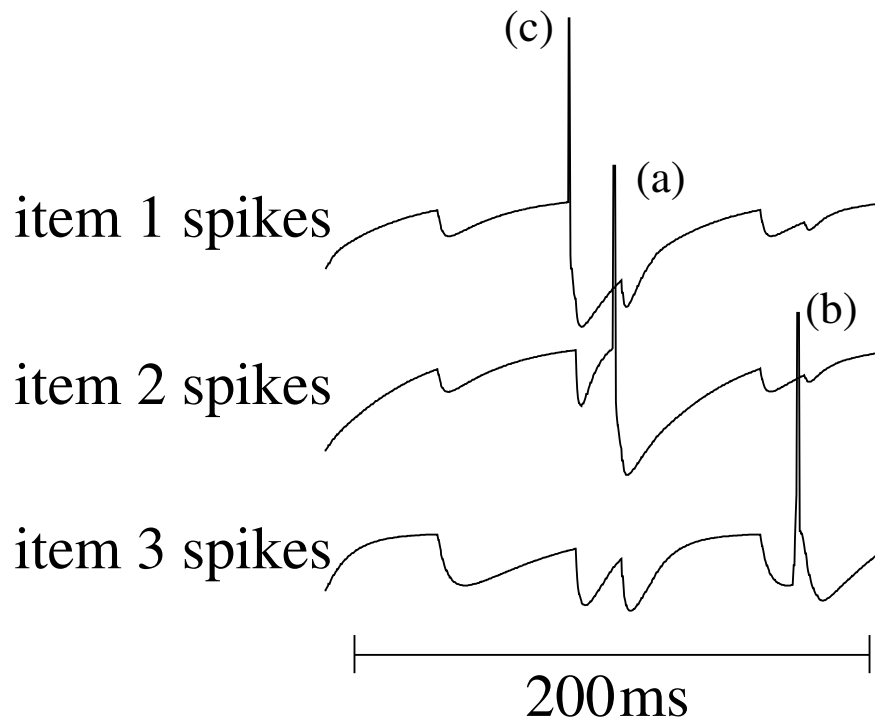


Figure 1

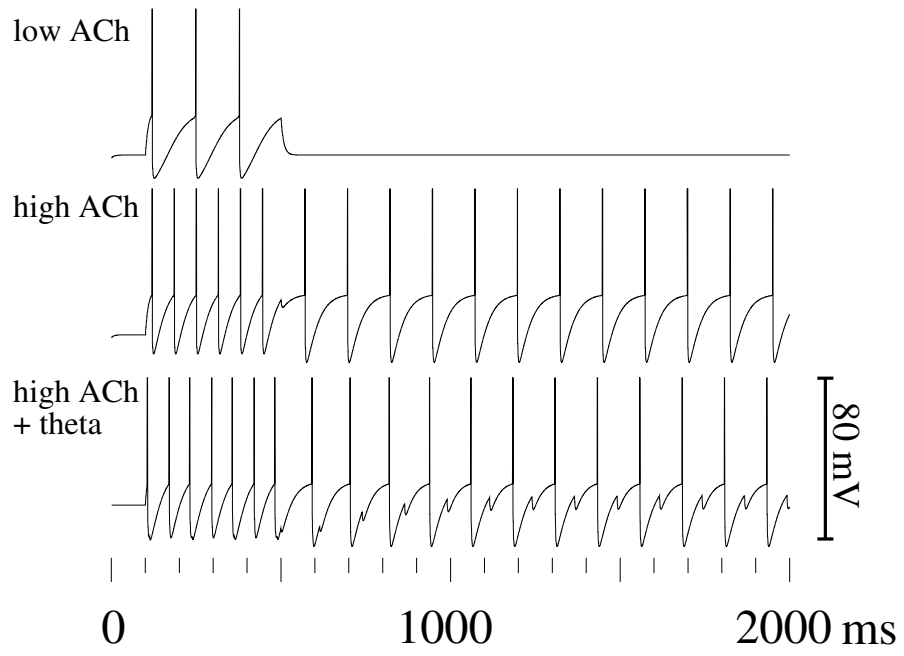


Figure 2

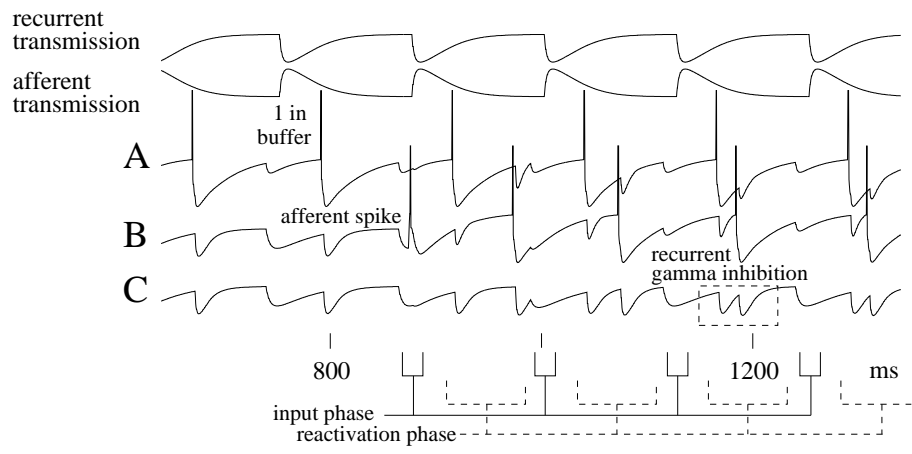


Figure 3

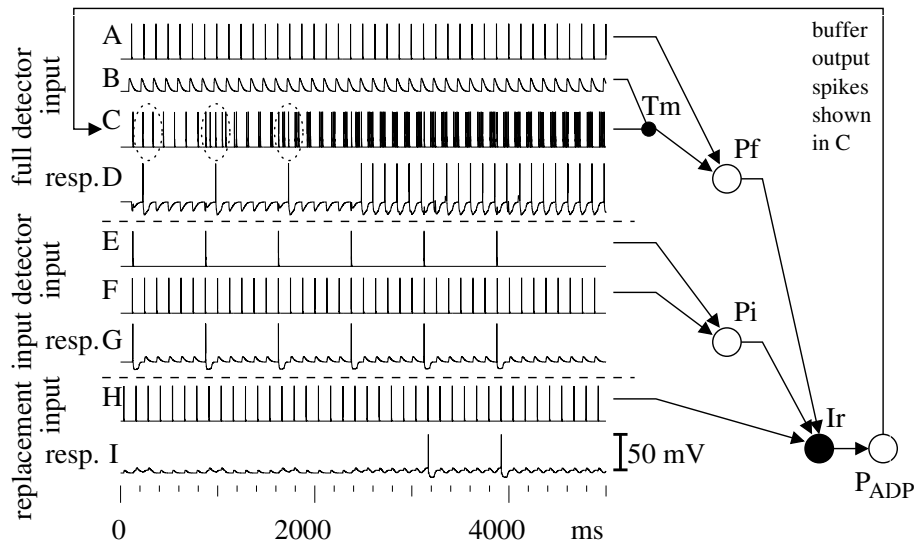


Figure 4

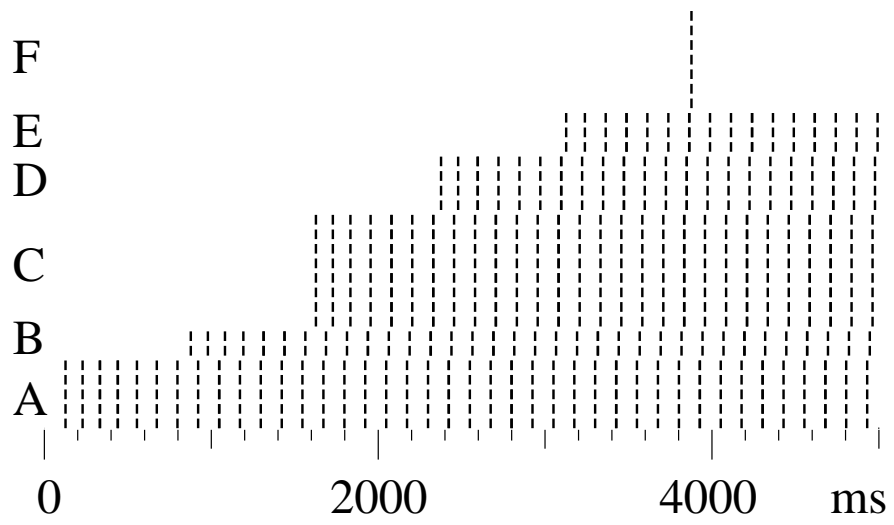


Figure 5

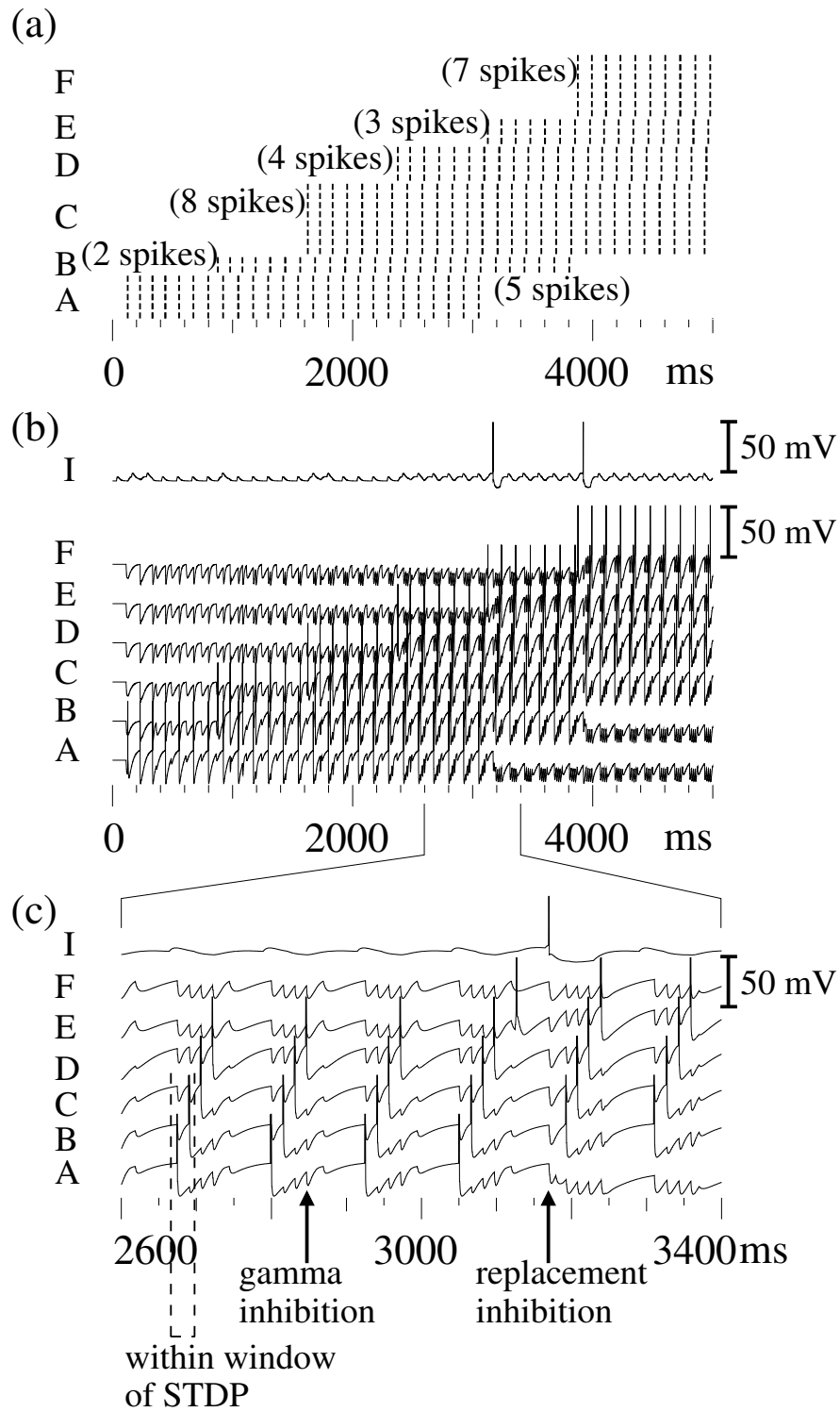


Figure 6

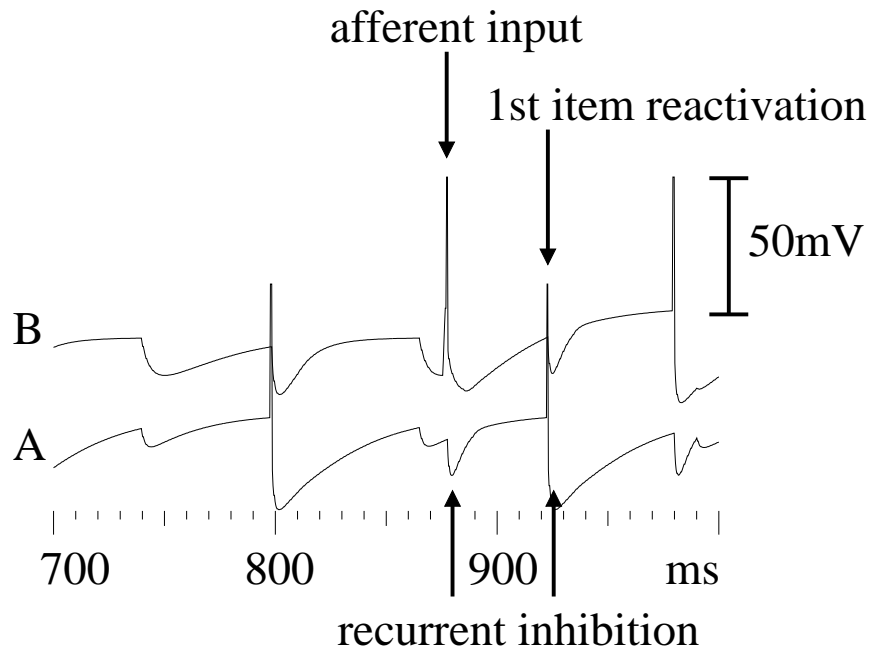


Figure 7

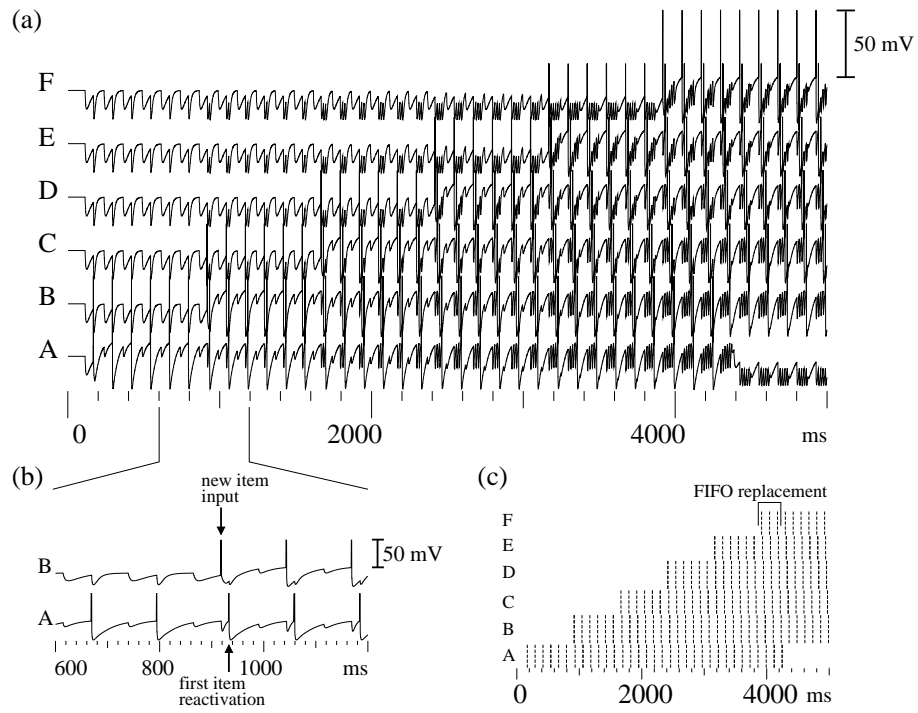


Figure 8

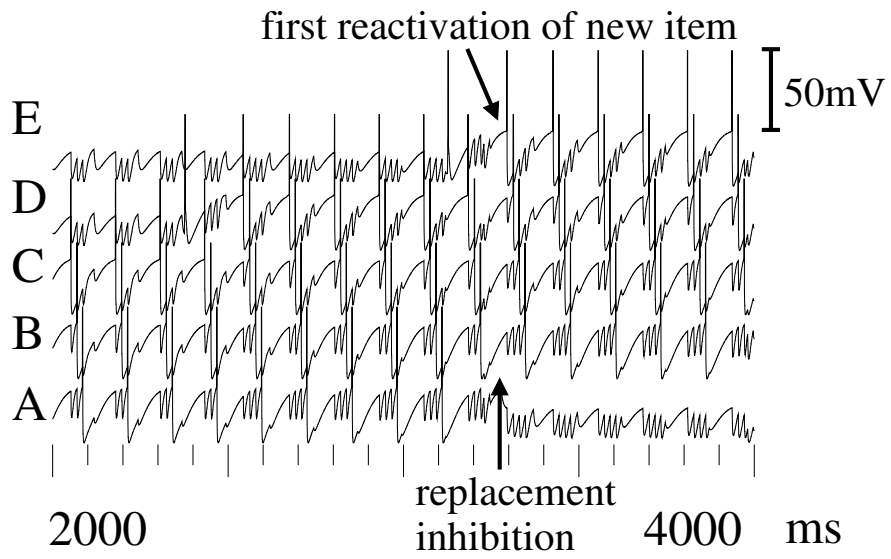


Figure 9

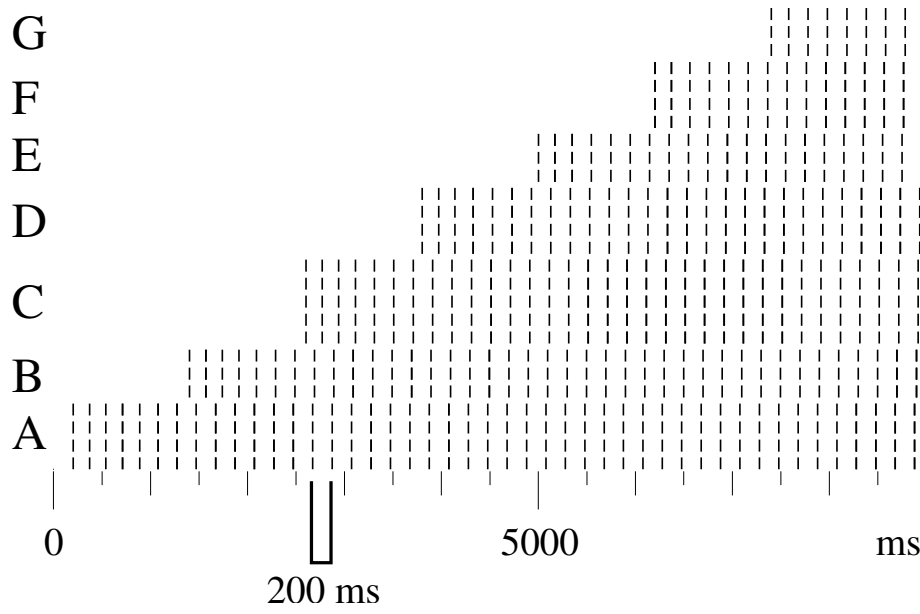


Figure 10

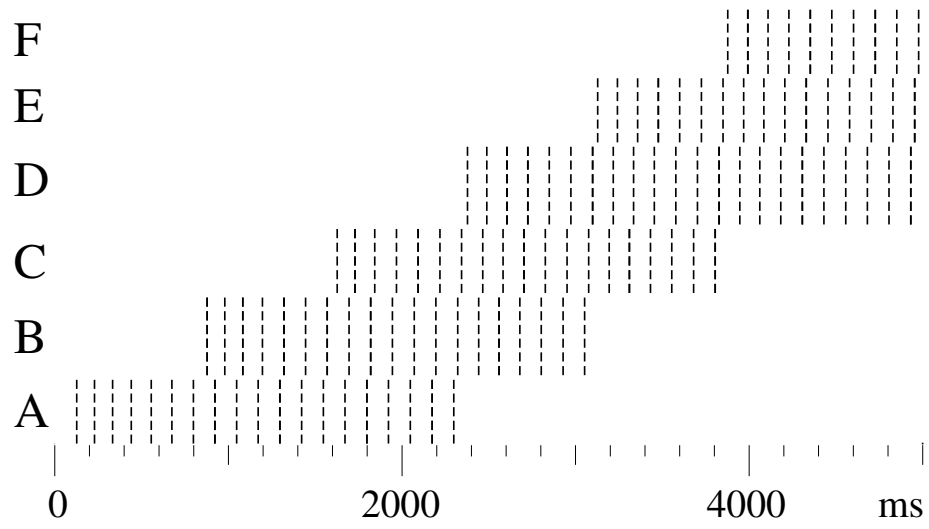


Figure 11

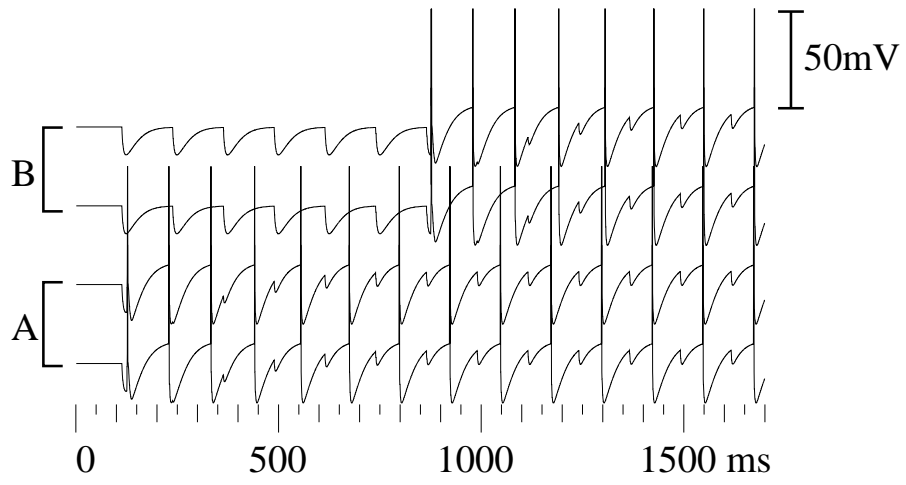


Figure 12

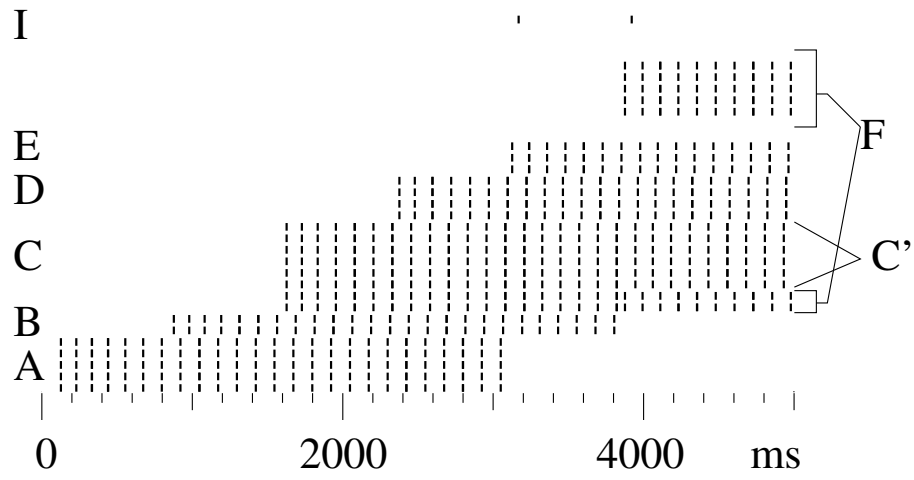


Figure 13

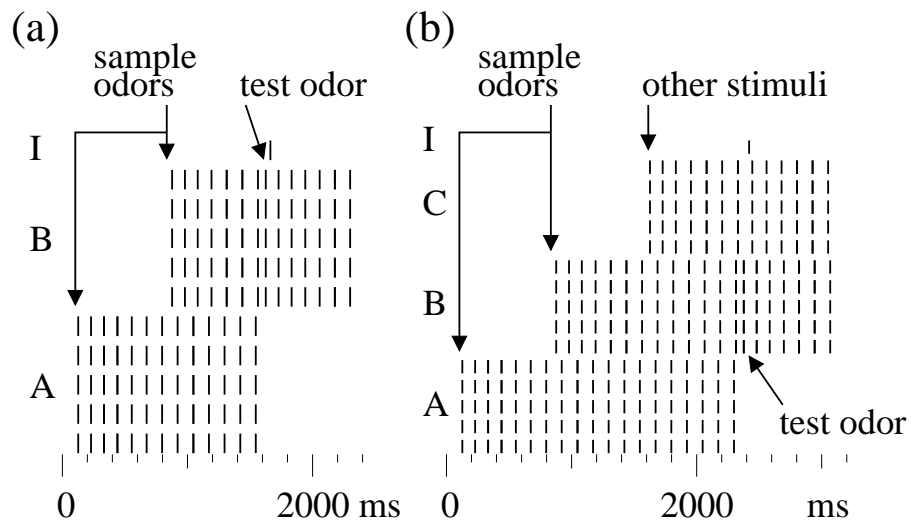


Figure 14

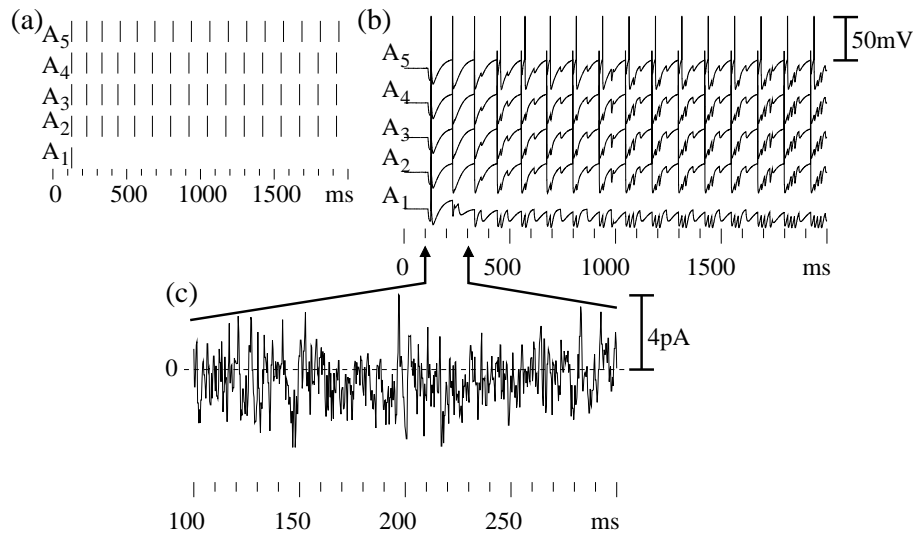


Figure 15

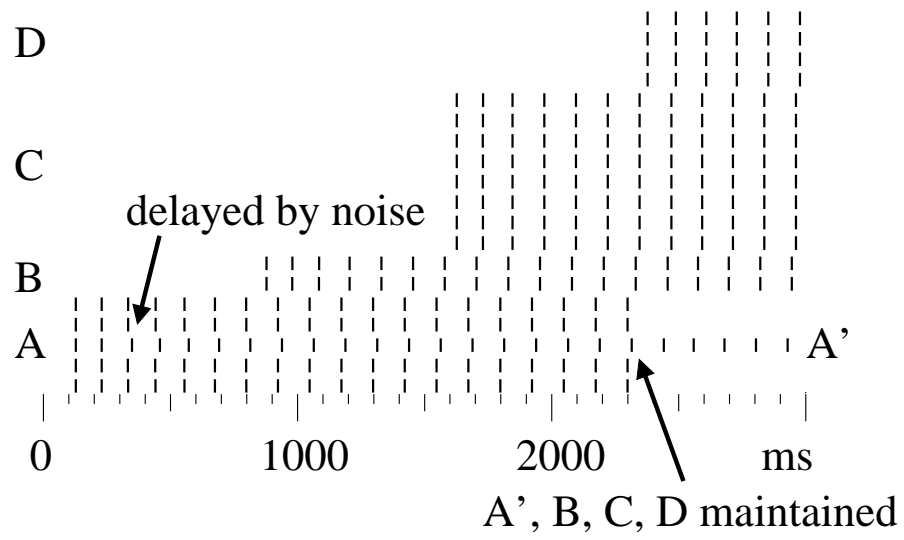


Figure 16

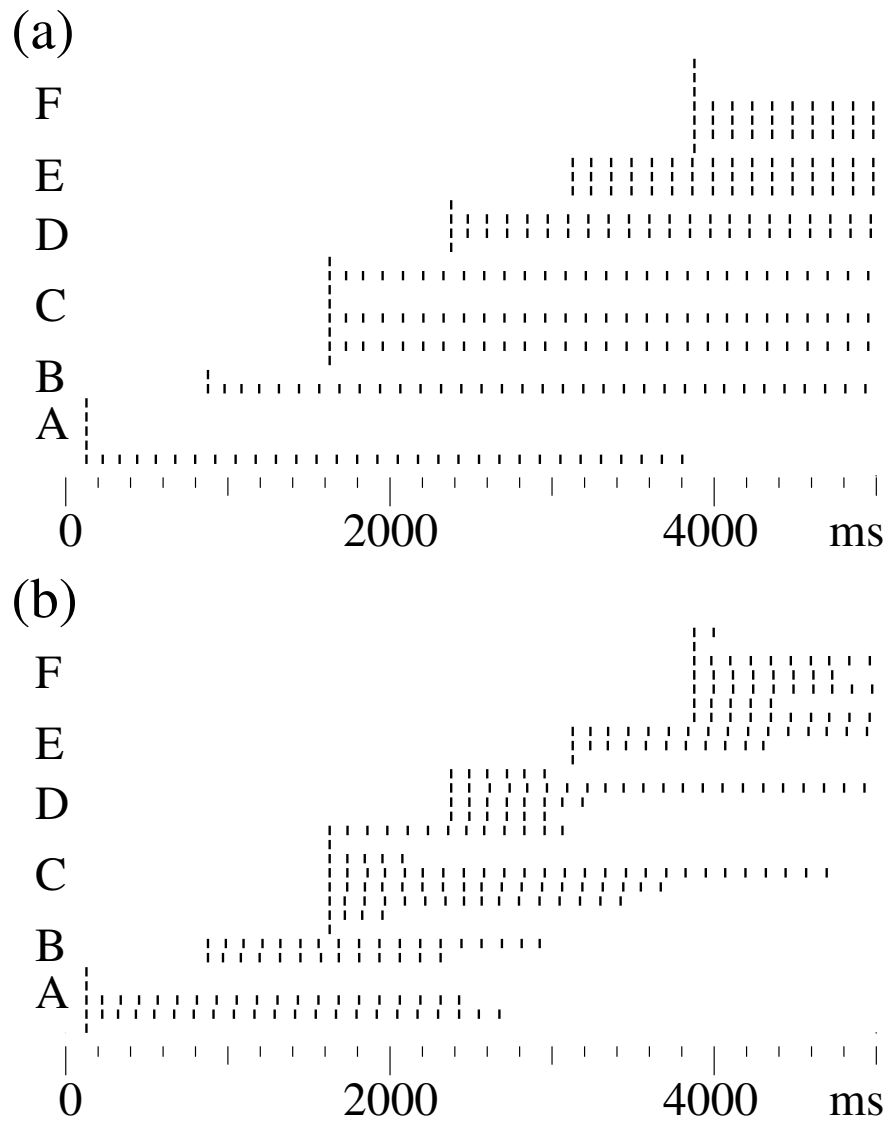


Figure 17